Neuron, Vol. 47, 29–41, July 7, 2005, Copyright ©2005 by Elsevier Inc. DOI 10.1016/j.neuron.2005.06.005

p53 Mediates Cellular Dysfunction and Behavioral Abnormalities in Huntington's Disease

Byoung-Il Bae,[1] Hong Xu,[2] Shuichi Igarashi,[3] Masahiro Fujimuro,[4] Nishant Agrawal,[1] Yoichi Taya,[7] S. Diane Hayward,[4] Timothy H. Moran,[3] Craig Montell,[1,2] Christopher A. Ross,[1,3,5] Solomon H. Snyder,[1,3,6] and Akira Sawa[1,3,*]

[1]Department of Neuroscience
[2]Department of Biological Chemistry
[3]Department of Psychiatry and Behavioral Sciences
[4]Department of Oncology
[5]Department of Neurology
[6]Department of Pharmacology and Molecular Science
Johns Hopkins University School of Medicine
725 North Wolfe Street
Baltimore, Maryland 21205
[7]Radiobiology Division
National Cancer Center Research Institute
Tokyo 104-0045
Japan

Summary

We present evidence for a specific role of p53 in the mitochondria-associated cellular dysfunction and behavioral abnormalities of Huntington's disease (HD). Mutant huntingtin (mHtt) with expanded polyglutamine (polyQ) binds to p53 and upregulates levels of nuclear p53 as well as p53 transcriptional activity in neuronal cultures. The augmentation is specific, as it occurs with mHtt but not mutant ataxin-1 with expanded polyQ. p53 levels are also increased in the brains of *mHtt* transgenic (*mHtt-Tg*) mice and HD patients. Perturbation of p53 by pifithrin-α, RNA interference, or genetic deletion prevents mitochondrial membrane depolarization and cytotoxicity in HD cells, as well as the decreased respiratory complex IV activity of *mHtt-Tg* mice. Genetic deletion of *p53* suppresses neurodegeneration in *mHtt-Tg* flies and neurobehavioral abnormalities of *mHtt-Tg* mice. Our findings suggest that p53 links nuclear and mitochondrial pathologies characteristic of HD.

Introduction

Huntington's disease (HD) is a genetically dominant neurodegenerative disease caused by a mutation in the *huntingtin* gene leading to an abnormal Huntingtin protein product (Htt) (The Huntington's Disease Collaborative Research Group, 1993). Mutant Htt protein (mHtt) contains elongated polyglutamines (polyQ) whose length correlates with an earlier age of disease onset (Ross, 2002; Sawa, 2001; Tobin and Signer, 2000). Expression of mHtt, especially N-terminal fragments, elicits cytotoxicity in cell models (Cooper et al., 1998; Hackam et al., 1998; Wellington et al., 2000) as well as fly models (Jackson et al., 1998; Marsh et al., 2000) and elicits behavioral abnormalities in mice (Carter et al., 1999; Hodgson et al., 1999; Reddy et al., 1998; Schilling et al., 1999), suggesting that the pathophysiology of HD involves a toxic gain of function.

The pathophysiology of HD has been linked to mitochondrial dysfunction (Grunewald and Beal, 1999; Sawa, 2001; Schapira, 1997). Mitochondrial enzyme activities of the respiratory chain complexes II/III and IV are impaired specifically in the caudate and putamen of HD patient brains (Browne et al., 1997; Tabrizi et al., 1999) and striatum of *mHtt* transgenic (*mHtt-Tg*) mice (Tabrizi et al., 2000). 3-Nitropropionic acid (3-NPA), a selective mitochondrial toxin for the complex II, elicits striatal damage resembling HD (Beal et al., 1993). Mitochondrial disturbances in HD patient brains are not likely secondary to overall neuropathologic alterations, as lymphoblasts from HD patients manifest abnormal mitochondrial membrane depolarization (Panov et al., 2002; Sawa et al., 1999). The mitochondrial defect may be disease specific, as lymphoblasts from the patients with spinocerebellar ataxia type 1 (SCA1), another neurodegenerative condition caused by an expanded polyQ in the disease gene *ataxin-1*, do not display mitochondrial membrane depolarization (Sawa et al., 1999).

Nuclear disturbances are also implicated in HD (Hodgson et al., 1999; Peters et al., 1999; Saudou et al., 1998; Schilling et al., 2004; Steffan et al., 2000; Wheeler et al., 2000). In both HD cell and transgenic animal models, nuclear accumulation of mHtt strongly enhances neurotoxicity. Mutant Htt interacts with nuclear factors such as CREB binding protein (CBP) (Nucifora et al., 2001) and Sp1/TAFII130 (Dunah et al., 2002), whose loss of function may mediate cytotoxicity.

The tumor suppressor gene *p53* has multiple functions in processes as diverse as angiogenesis and chemotaxis (Vogelstein et al., 2000). p53 is also expressed in the central nervous system (CNS), where its function is not established (Morrison and Kinoshita, 2000). While acute excitotoxic insults, such as kainic acid, induce p53 activation and *p53* null mice are mildly resistant to neurotoxicity (Morrison et al., 1996), it is unclear whether the increase of p53 is primary or secondary to excitotoxicity. Overexpression of p53 in dissociated primary neuron cultures elicits neuronal death (Jordan et al., 1997), but the role of endogenous p53 has not been investigated. Binding of mHtt with p53 has been reported (Steffan et al., 2000), but its pathophysiological implication remains unknown. Immortalized striatal neurons derived from *mHtt* knockin mouse embryos show elevated levels of p53 protein (Trettel et al., 2000). Genes regulated by p53 are among a large cohort upregulated in cell cultures transfected with *mHtt* (Sipione et al., 2002).

Although nuclei and mitochondria participate in HD pathology, their relationship has been elusive. Because nuclear p53 regulates many mitochondrial genes and genes for oxidative stress (Sharpless and DePinho, 2002; Vogelstein et al., 2000), we hypothesized that p53 might link the nuclear and mitochondrial pathologies in HD.

*Correspondence: asawa1@jhmi.edu

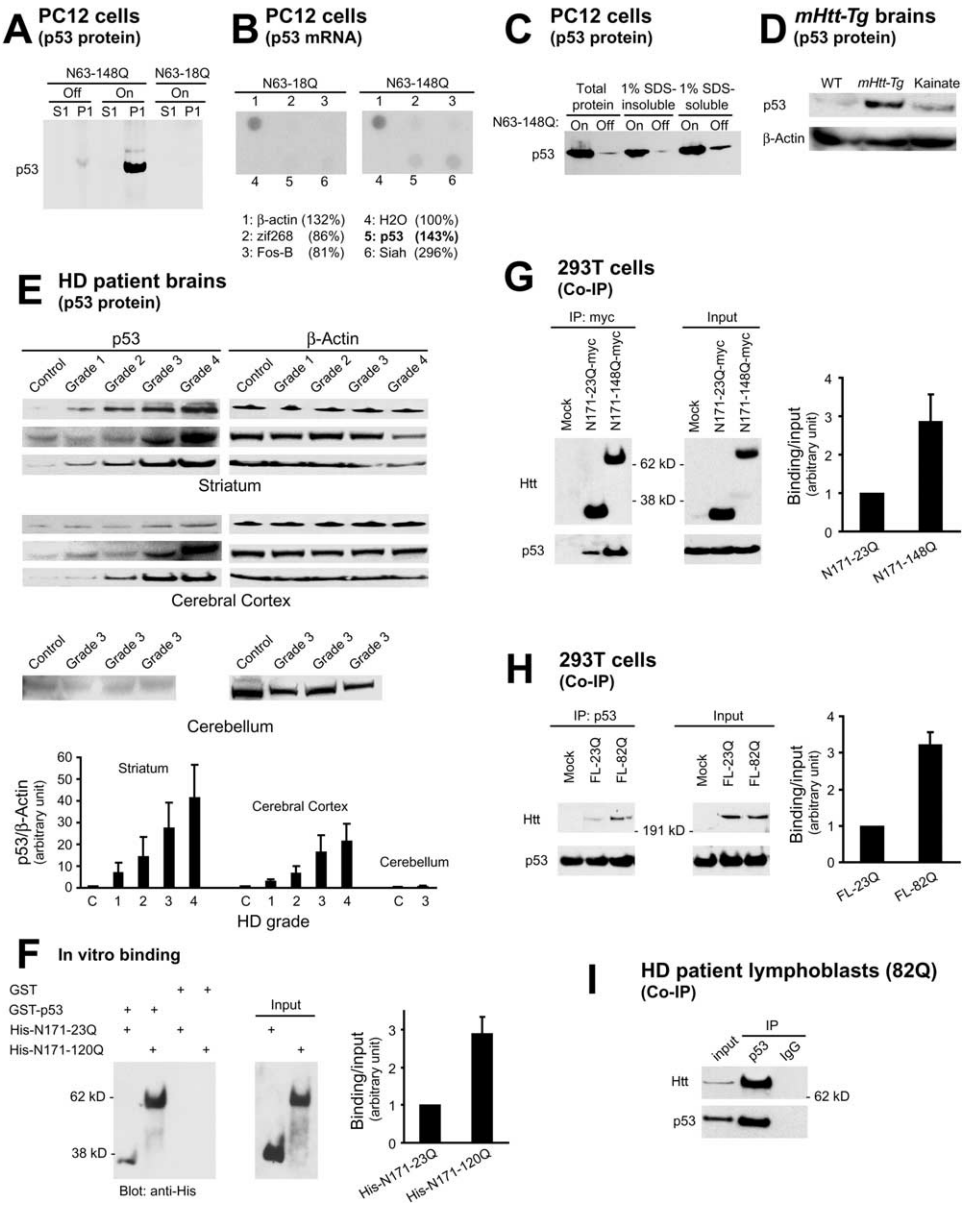

Figure 1. mHtt Upregulates p53

(A) Immunoblotting shows that p53 protein level is increased significantly in the P1 fraction of PC12 cells stably expressing the N-terminal 63 amino acids of Htt with 148 polyglutamine (N63-148Q), but not the cells expressing N63-18Q, after 5 days of induction. Inhibition of N63-148Q induction is not associated with p53 upregulation.

(B) p53 mRNA level is only marginally changed by mHtt, as shown by reverse Northern dot blotting. The mRNA expression ratios in cells with N63-148Q to those with N63-18Q are 132% (β-actin), 86% (zif268), 81% (Fos-B), 100% (H_2O), 143% (p53), and 296% (Siah).

(C) p53 protein level is increased both in 1% SDS-soluble and -insoluble fractions of PC12 cells stably expressing Htt N63-148Q, which is shown by immunoblotting.

(D) Increased p53 protein level is evident in immunoblotting from the whole-cell lysates of striatum of 8-month-old *mHtt-Tg* mouse expressing the N-terminal 171 amino acids of Htt with 82 polyglutamine (N171-82Q), compared to wild-type (WT) littermate. Injection of kainate elicits a lesser increase of p53 than mHtt. n = 3 per each group.

(E) p53 is increased in whole tissue lysates of postmortem cerebral cortex and striatum of HD patients, which is shown by immunoblotting. The increase in p53 protein level is greater in cases with higher grades of HD pathology. No increase of p53 by mHtt is evident in the cerebellum. C, control (n = 3 per each grade).

(F) p53 directly binds to Htt. His-Htt N171-23Q or -120Q, and GST-p53 purified from bacteria were incubated in PBS containing 1% Triton X-100. His-Htt bound to GST-p53 was analyzed by immunoblotting.

(G and H) Expansion of polyQ strengthens the interaction between exogenous Htt and p53. Co-IP of Htt and p53 was examined in 293T cells transfected with (G) N-terminal *Htt* (N171-23Q-myc or N171-148Q-myc) or (H) full-length *Htt* (FL-23Q or FL-82Q).

(I) In HD lymphoblasts treated with staurosporine, endogenous p53 and Htt interact, which is evidenced by coprecipitation of Htt with p53 by an anti-p53 antibody, but not by IgG.

All the figures represent two to three independent experiments. The results of the experiments in (E)–(H) are quantified in arbitrary units, where 1 equals to level of control or wtHtt.

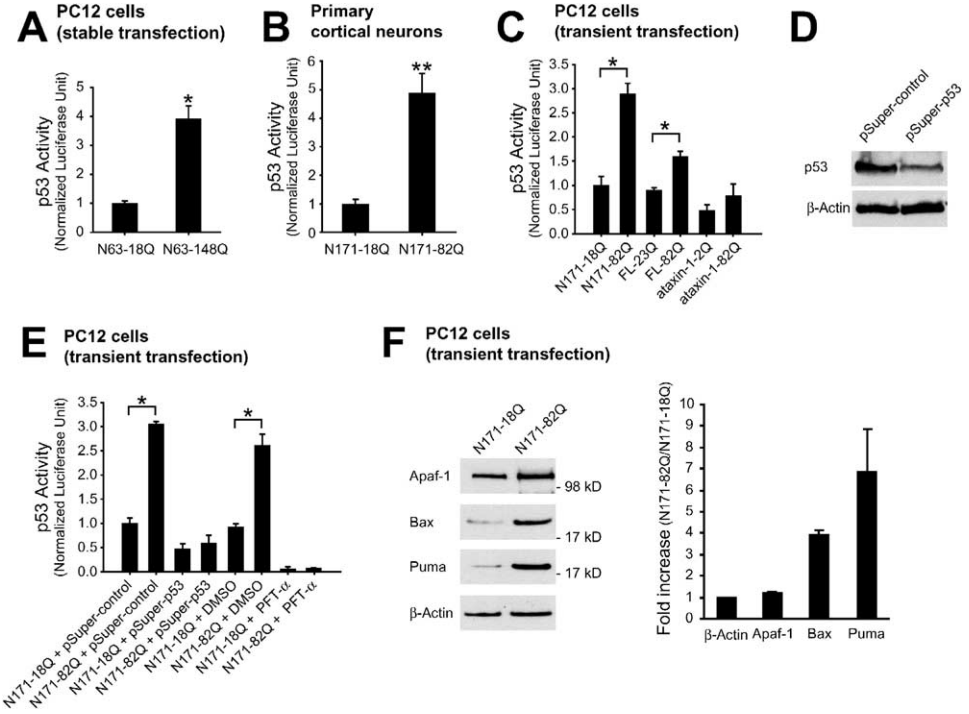

Figure 2. mHtt Increases p53-Mediated Transcription

(A) Stably transfected N63-148Q increases p53 transactivation 4-fold in PC12 cells compared to N63-18Q (t test: *p < 0.0005).

(B) Transiently transfected N171-82Q increases p53 transactivation 5-fold in rat primary cortical neurons compared to N171-18Q (t test: **p < 0.0001).

(C) Unlike N171 and full length (FL) Htt, transiently transfected ataxin-1 does not increase p53 transcription activity, (t test: *p < 0.0005).

(D) RNAi to p53 (pSuper-p53) knocks down p53 protein, whereas control RNAi (pSuper-control) does not.

(E) RNAi to p53 and pifithrin-α (PFT-α) effectively inhibit p53-mediated transcription (t test: *p < 0.0005).

(F) p53 target proteins are significantly augmented by mHtt. Apaf-1, Bax, and Puma levels were examined in PC12 cells transiently transfected with *Htt* N171-18Q or N171-82Q 90 hr after transfection. Bax and Puma protein levels were augmented 4-fold and 6-fold, respectively, whereas Apaf-1 level was only marginally changed.

All the graphs show mean ± SEM of three independent experiments performed in triplicate.

We have investigated p53 in HD cell and transgenic animal models expressing mHtt as well as HD patient brains. We present evidence for a specific role of p53 in the mitochondria-associated cellular dysfunction and behavioral abnormalities of Huntington's disease.

Results

Mutant Htt Upregulates Nuclear p53 Levels and Transcription Activity

In PC12 cells stably expressing the N-terminal 63 amino acids of Htt with 148 polyQ (N63-148Q) in an inducible manner (Igarashi et al., 2003), the protein level of p53 is increased more than 10-fold after induction of mHtt, but not wild-type Htt (wtHtt) N63-18Q. The increased p53 occurs selectively in the P1 fractions designated as crude nuclei (Figure 1A) in 1% SDS-soluble, nonaggregate fractions (Figure 1C), implying that the transactivation-independent role for p53 in the mitochondria is unlikely (Chipuk et al., 2004). The increase of p53 protein appears to be posttranslational, as mRNA levels of p53 are increased only 1.4-fold (Figure 1B). In the brains of transgenic mice expressing the N-terminal 171 amino acids of Htt with 82 polyglutamine repeats (N171-82Q) (Schilling et al., 1999), p53 is also elevated (Figure 1D). Enhancement of p53 is selective, as kainate, which causes more neuronal death than mHtt, induces a lesser increase in p53. Postmortem brains of human HD patients also manifest substantial p53 increases, with the highest levels in the cases with the most extensive HD pathology (Figure 1E). Only striatum and cerebral cortex show p53 upregulation with no increase in cerebellum, fitting with the regional and cellular selectivity of HD pathology (Sawa, 2001; Sisodia, 1998; Tobin and Signer, 2000).

Confirming the previously reported interaction between exon 1 of Htt (N63-20Q, -51Q, and -83Q) and p53 (Steffan et al., 2000), we observe direct binding of Htt N171 and p53 in vitro (Figure 1F). Furthermore, p53 coimmunoprecipitates with N171 as well as full-length (FL) Htt in transiently transfected 293T cells (Figures 1G and 1H). In both cases, mHtt binds more efficiently to p53 than wtHtt. Coimmunoprecipation (co-IP) of p53 and Htt at endogenous protein levels is evident in stressed HD patient lymphoblasts (Figure 1I).

We wondered whether augmented p53 is associated with increased transcriptional activity. Using the p53 binding sequence upstream of a luciferase reporter gene (el-Deiry et al., 1992), we monitored p53-mediated

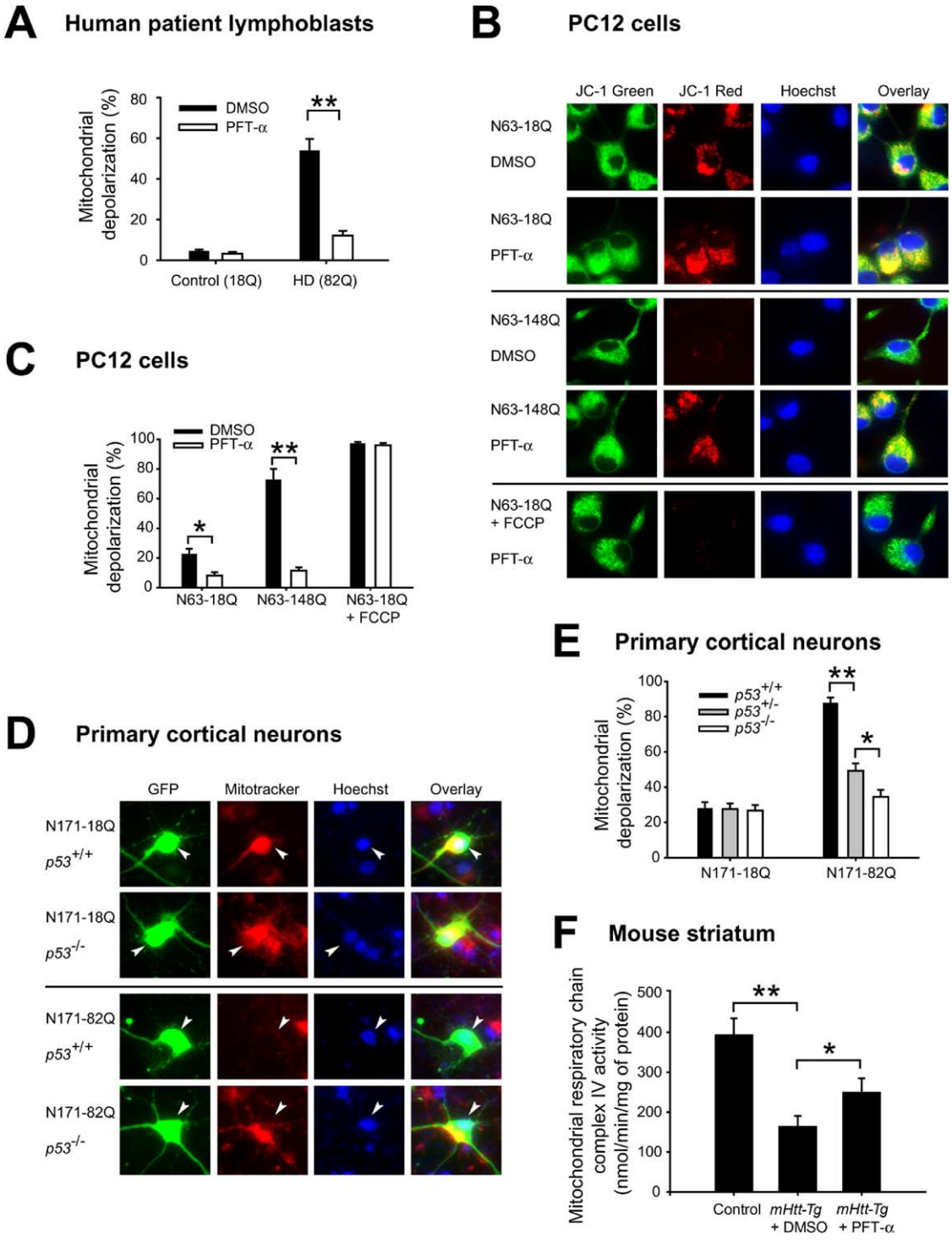

Figure 3. Suppression of p53 Reverses mHtt-Elicited Mitochondrial Depolarization

(A) Pretreatment with 10 μM pifithrin-α (PFT-α) reverses mitochondrial depolarization in 25 μM cyanide-exposed HD patient lymphoblasts (82 polyQ). In response to cyanide, only HD, but not control (18 polyQ), lymphoblasts manifest robust mitochondrial depolarization (t test: **p < 0.0001).

(B and C) Suppression of p53 by PFT-α reverses mitochondrial depolarization elicited by N63-148Q in PC12 cells. Cells were evaluated on the fifth day of induction. JC-1 produces a red signal from polarized mitochondria and green from depolarized mitochondria. Mitochondria are polarized in PC12 cells expressing N63-18Q and depolarized in cells with N63-148Q, reflecting initiation of cell death, which is reversed by pifithrin-α. Pifithrin-α does not protect the cells from rapid mitochondrial depolarization by FCCP, an uncoupler of mitochondrial respiration Each graph bar corresponds to the scoring of about 500 PC12 cells from randomly chosen fields (t test: **p < 0.0001, *p < 0.005).

(D and E) Genetic deletion of *p53* prevents mitochondrial depolarization by N171-82Q in mouse primary cortical neurons. After 72 hr incubation

gene activation (Figures 2A and 2B). Stable expression of *mHtt* N63-148Q in PC12 cells elicits a 4-fold increase of p53 transcriptional activation, while in rat primary cortical cultures, transient transfection of mHtt N171-82Q causes an approximately 5-fold amplification of p53 activity. Activation is selective for N171-82Q as well as FL mHtt, since transient expression of ataxin-1 with expanded polyQ fails to influence p53 transcriptional activity (Figure 2C). Vector-based RNA interference (RNAi) to p53 (pSuper-p53) (Brummelkamp et al., 2002) and a specific p53 inhibitor, pifithrin-α (1 μM) (Duan et al., 2002; Komarov et al., 1999), both block mHtt-induced p53 transactivation (Figures 2D and 2E). We compared protein levels of three p53 targets that directly associate with mitochondria, Apaf-1 (Sang et al., 2005), Bax (Miyashita and Reed, 1995), and Puma (Yu et al., 2001), in *Htt*-transfected PC12 cells. Bax and Puma protein levels are significantly augmented by mHtt, whereas Apaf-1 is only marginally augmented (Figures 2F).

Augmented p53 Mediates Mitochondrial Dysfunction in HD Cell and Transgenic Animal Models

Mitochondrial membrane depolarization is enhanced in lymphoblasts of HD but not SCA1 patients treated with low concentrations of cyanide (25 μM) (Sawa et al., 1999). As p53 can mediate mitochondrial function and is selectively influenced by mHtt but not by mutant ataxin-1 (Figure 2C), we explored a role for p53 in mHtt-mediated mitochondrial dysfunction.

Pretreatment of the cyanide-exposed HD lymphoblasts with 10 μM pifithrin-α blocks depolarization of the mitochondria (Figure 3A). Induction of mHtt N63-148Q in PC12 cells causes pronounced mitochondrial membrane depolarization after 5 days of induction (Figures 3B and 3C). Treatment with pifithrin-α (1 μM) completely blocks the depolarization, indicating that p53 mediates the mitochondrial abnormality. By contrast, pifithrin-α does not affect the rapid mitochondrial membrane depolarization elicited by carbonylcyanide p-(trifluoromethoxy) phenylhydrazone (FCCP), a protonophore and uncoupler of oxidative phosphorylation in mitochondria, demonstrating specificity of pifithrin-α for the p53 pathway.

In primary cortical cultures of $p53^{+/+}$ mice, we observe substantial mitochondrial membrane depolarization associated with transfected *mHtt* N63-148Q but not *wtHtt* N63-18Q at a time when nuclei are intact in most neurons (Figures 3D and 3E). Cultures from $p53^{+/-}$ and $p53^{-/-}$ mice (Donehower et al., 1992) are protected from this mitochondrial depolarization.

mHtt-Tg mouse models display mitochondrial dysfunction affecting enzymes in the mitochondrial respiratory chain IV (Tabrizi et al., 2000). To evaluate the influence of p53 on such mitochondrial dysfunction in vivo, we injected line 81 N171-82Q *mHtt-Tg* mice i.p. with pifithrin-α, which efficiently crosses the blood-brain barrier (Duan et al., 2002). The treatment significantly prevents impaired complex IV activity of *mHtt-Tg* mice (Figure 3F).

p53 Mediates mHtt Cytotoxicity, Independent of Nuclear Aggregate Formation

To address the cellular consequences of mitochondrial dysfunction, we evaluated cytotoxicity following inhibition of p53 with pifithrin-α, RNAi, or genetic deletion. Induction of mHtt N63-148Q (Igarashi et al., 2003) or transfection of FL-82Q causes the death of PC12 cells. The tripling of PC12 cell death elicited by mHtt is abolished by pifithrin-α (10 μM) or pSuper-p53 (Figure 4A). Antisense oligonucleotides against p53 provide about the same degree of protection as pifithrin-α (data not shown).

We also employed primary cerebral cortical cultures from wild-type and *p53*-deleted mice. In $p53^{+/+}$ cultures, *mHtt* N171-82Q transfection elicits 2.5 times greater cell death than *wtHtt* N171-18Q. By contrast, mHtt fails to elicit neurotoxicity in cultures from $p53^{-/-}$ mice. Pronounced, but not complete, protection is also evident in $p53^{+/-}$ cultures (Figures 4B and 4C).

We investigated whether p53 is also involved in mHtt-associated aggregate formation (DiFiglia et al., 1997), whose role in HD pathogenesis is controversial (Arrasate et al., 2004; Sisodia, 1998). We monitored the formation and nuclear targeting of mHtt aggregates in cortical cultures (Figures 4D and 4E). We find no significant difference between $p53^{+/+}$ and $p53^{-/-}$ neurons in aggregate formation and nuclear localization of mHtt. We observe substantial nuclear fragmentation and condensation in $p53^{+/+}$ but not in $p53^{-/-}$ preparations of mHtt cells. Thus, in contrast to the critical role of p53 in mitochondrial membrane depolarization and cell death, mHtt-associated nuclear aggregate formation does not appear to be influenced by p53.

Deletion of p53 Suppresses mHtt-Induced Retinal Degeneration in *Drosophila*

To explore the role of p53 in mHtt-induced cell death of intact animals, we evaluated the effect of p53 deletion in *mHtt-Tg* flies (Jackson et al., 1998). The *mHtt-Tg* flies, which express mHtt N170-120Q under the control of the eye-specific expression GMR promoter (Hay et al., 1994), manifest prominent cell death of photoreceptor neurons. We crossed *mHtt-Tg* flies with *p53* mutant flies in which the *p53* gene was deleted by homologous recombination (Rong et al., 2002) and assessed the effects of deleting *p53* in the compound eyes. Wild-type compound eyes contain ~800 ommatidia, each of

of Htt with GFP, changes in mitochondrial membrane potential were measured using red emission of a fluorescent indicator, Mitotracker. N171-82Q causes mitochondrial depolarization in $p53^{+/+}$ but not in $p53^{-/-}$ neurons. Cell death is not evident at 72 hr, as shown by long neurites (GFP) and round nuclei (Hoechst). Each graph bar corresponds to the scoring of about 1000 to 2000 neurons from randomly chosen fields (t test: $^{**}p < 0.0001$, $^{*}p < 0.001$).

(F) Specific activity of mitochondrial respiratory chain complex IV, cytochrome C oxidase, is decreased in *mHtt-Tg* mouse striatum, which is significantly reversed by daily i.p. administration of pifithrin-α. Four brains per group were analyzed (t test: $^{*}p < 0.01$, $^{**}p < 0.005$). All the graphs and figures represent two to three independent experiments. Bars show mean ± SEM.

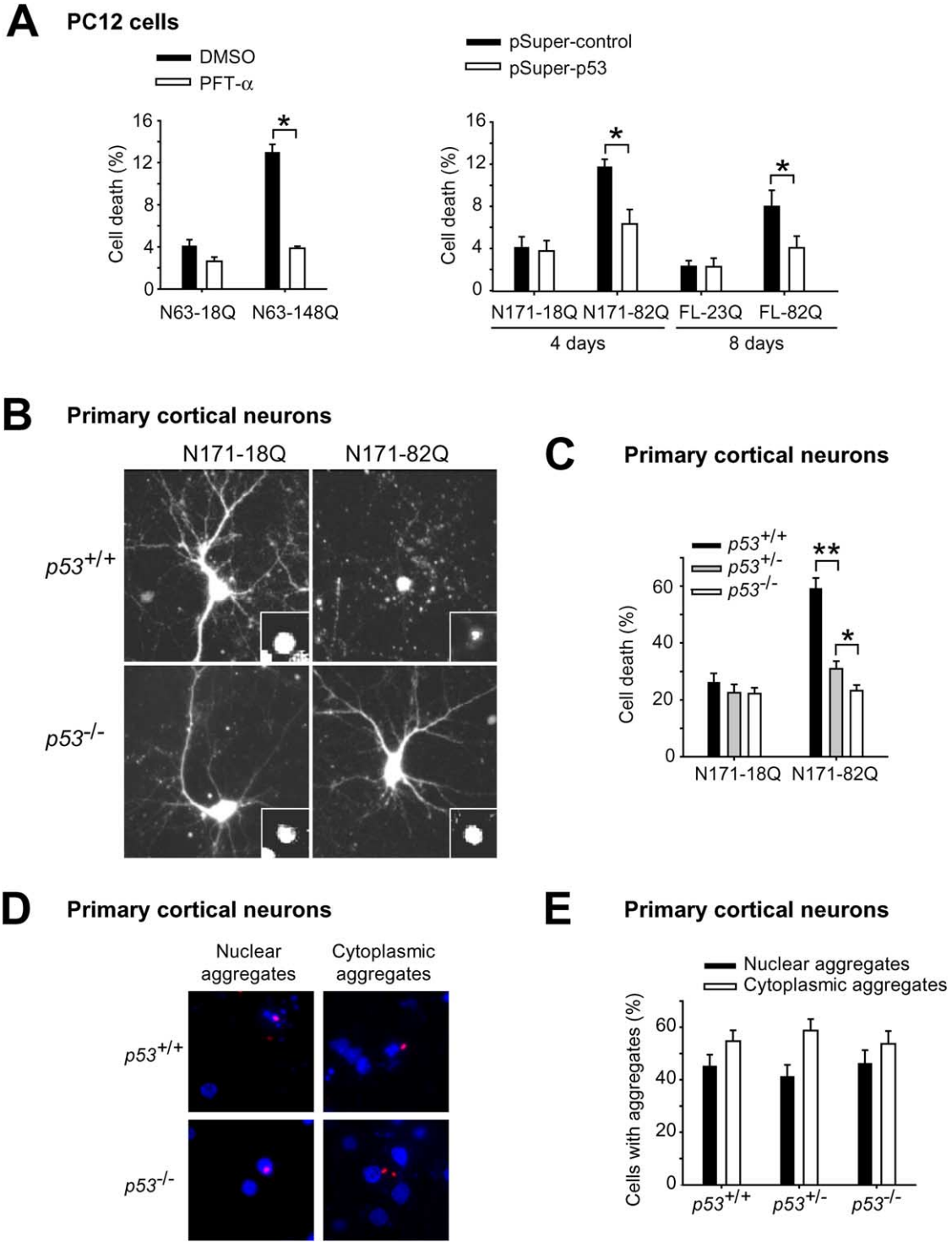

Figure 4. Suppression of p53 Reverses Cell Death by mHtt

(A) Suppression of p53 prevents toxicity by mHtt in PC12 cells. Pifithrin-α (PFT-α) prevents N63-148Q toxicity on the 8th day of induction (the left panel). RNAi to p53 blocks N171-82Q and FL-82Q toxicity 4–8 days after transient transfection (the right panel). (t test: *p < 0.001).

(B and C) Mouse primary cortical neurons nullizygous for *p53* are resistant to N171-82Q toxicity. *Htt* was cotransfected with GFP on 4 DIV, and toxicity was measured after 96 hr of incubation. Neuronal degeneration was assessed by neurite loss and nuclear shrinkage. (Inset) Hoechst nuclear staining (B). Homozygous deletion of *p53* reverses mHtt-mediated cellular toxicity in cortical neurons. Pronounced protection is also evident in $p53^{+/-}$ cultures (t test: **p < 0.0001, *p < 0.001).

(D and E) p53 does not affect mHtt aggregate formation. N67-104Q tagged with GFP (N67-104Q-GFP) was transfected into cortical neurons on 4 DIV. Nuclei are shown in blue by Hoechst staining. N67-104Q-GFP is pseudocolored in red. All the transfected neurons develop nuclear or cytoplasmic mHtt aggregates after 2 days of incubation, regardless of p53 genotype. Nuclear fragmentation reflecting apoptosis is evident in $p53^{+/+}$ neurons but absent in $p53^{-/-}$.

All the graphs and figures represent four independent experiments. Bars show mean ± SEM. Each graph bar corresponds to the scoring of about 1000 to 2000 neurons or 500 PC12 cells from randomly chosen fields.

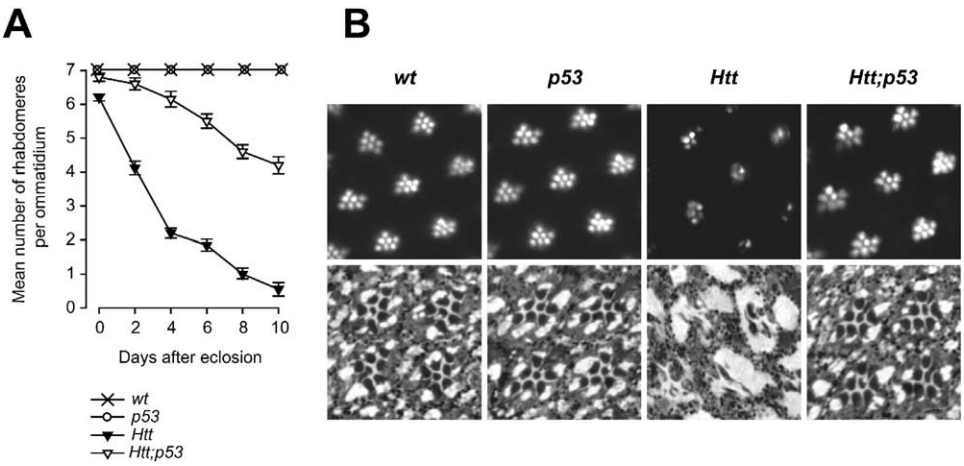

Figure 5. Genetic Deletion of *p53* Diminishes Retinal Degeneration in *mHtt-Tg Drosophila*

(A) Time course of photoreceptor degeneration determined by the optical neutralization technique. GMR-driven mHtt N170-120Q causes age-dependent retinal degeneration in *Drosophila* (*Htt*). Genetic deletion of *p53* provides substantial, but not complete, protection from degeneration (*Htt;p53*). No photoreceptor cell loss is observed in wild-type (wt) and *p53* knockout (*p53*) flies. Each point shows the mean ± SD.

(B) Representative photomicrographs of ommatidia using the optical neutralization (the upper panel) and Toluidine blue-stained semithin sections (the lower panel) from wt, *p53*, *Htt*, and *Htt;P53* flies at 4 days posteclosion.

which includes seven photoreceptor cells in any given plane of section. The photoreceptor cells contain a microvillar structure referred to as the rhabdomere. Wild-type (wt) and p53 knockout flies (*p53*) display a normal composition of seven photoreceptor cells in each ommatidium (Figure 5). *mHtt-Tg* flies (*Htt*), however, manifest strong age-dependent loss of rhabdomeres and photoreceptor cells, as reported previously (Jackson et al., 1998) (Figure 5). Deletion of two copies of *p53* in *mHtt-Tg* flies (*Htt;p53*) suppresses this phenotype, as shown using the optical neutralization technique on intact heads and in Toluidine blue-stained sections (Figure 5). Thus, p53 mediates mHtt-induced neurotoxicity in intact organisms.

p53 Modulates Neurobehavioral Abnormalities in HD Transgenic Mouse Models

Mutant *Htt* transgenic mice manifest several neurobehavioral abnormalities, presumably reflecting abnormalities in cortico-striato-pallido-thalamo-pontine neural pathways: clasping of the limbs, augmented circling behavior, impaired prepulse inhibition, and poor performance in rotarod tests (Braff et al., 2001; Carter et al., 1999; Hebb and Robertson, 1999; Hodgson et al., 1999; Reddy et al., 1998; Schilling et al., 1999). Prepulse inhibition of startle reflexes is also disordered in HD patients (Swerdlow et al., 1995). The rotarod paradigm is a widely used measure of motor coordination in HD mouse models. However, impairment in the rotarod test may not necessarily reflect striatal dysfunction, because mice with cerebellar deficits or muscle relaxation perform poorly in rotarod testing (Crawley, 2000).

To address a possible role for p53 in *mHtt-Tg* mice behavior, we genetically deleted the two alleles of *p53* in line 81 of *mHtt-Tg* mice overexpressing N171-82Q (Schilling et al., 1999) by cross-breeding with *p53* knockout mice.

When suspended by the tail, wild-type and $p53^{-/-}$ mice display escape reflexes (hindlimbs spread), whereas *mHtt-Tg* mice promptly clasp their hindlimbs (Sanchez et al., 2003; Schilling et al., 1999). In *mHtt-Tg*/$p53^{-/-}$ mice, this motor dysfunction is ameliorated (Figures 6A and 6B).

We observe a pronounced increase in a clockwise rotational behavior of 3- to 3.5-month-old line 81 *mHtt-Tg* mice in the open field test, as reported in other types of *mHtt-Tg* mice (Hodgson et al., 1999; Reddy et al., 1998) (Figure 6C). The increased rotation is selective, because time spent in the corner, reflecting "anxiety" (Crawley, 2000), as well as vertical exploratory movements are not affected in *mHtt-Tg* mice (data not shown). By contrast, rotation is not increased in *mHtt-Tg*/$p53^{-/-}$ mice (Figure 6C).

Startle responses to a loud 120 dB noise are inhibited by prior exposure of wild-type and $p53^{-/-}$ mice to a 2–4 dB noise. As observed with another line of *mHtt-Tg* mice (Carter et al., 1999), our *mHtt-Tg* mice display a 50%–65% decrease in this prepulse inhibition. This abnormality is not evident in *mHtt-Tg*/$p53^{-/-}$ mice (Figure 6D).

Confirming earlier work (Carter et al., 1999; Hodgson et al., 1999; Reddy et al., 1998; Schilling et al., 1999), *mHtt-Tg* mice display rotarod performance deficits, which are reversed in *mHtt-Tg*/$p53^{-/-}$ mice (Figure 6E).

Expression of mHtt N171-82Q in *mHtt-Tg* mice is under the control of mouse prion protein promoter (MoPrP) (Schilling et al., 1999) and not affected by genetic deletion of *p53* (Figure 6F). Body weights of *mHtt-Tg* mice are unaffected by *p53* deletion (Figure 6G).

Normalization of neurobehavioral deficits of *mHtt-Tg* mice by genetic deletion of *p53* indicates a role for p53 in the expression of these disturbances.

Discussion

In this study, we present evidence favoring a specific role for p53 in HD pathology. Mutant Htt binds p53 and

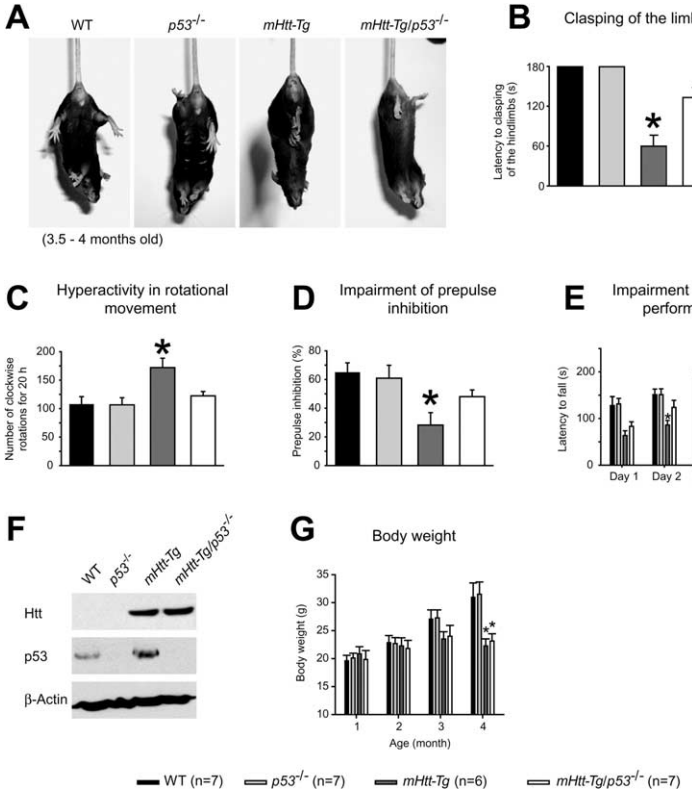

Figure 6. Genetic Deletion of *p53* Reverses Behavioral Abnormalities in *mHtt-Tg* mice

(A and B) Deletion of *p53* increases latency to clasping of the hindlimbs in *mHtt-Tg* mice. The latency was measured up to 3 min.

(C) Hyperactivity in rotational movement of 3- to 3.5-month-old *mHtt-Tg* mice is normalized by deletion of *p53*. Bars show the number of clockwise rotations for 20 hr in open-field test machines.

(D) Impairment of prepulse inhibition of the acoustic startle response in *mHtt-Tg* mice is reversed by deletion of *p53*. Bars indicate prepulse inhibition of mice responding to acoustic stimuli of 120 dB with 100 ms prepulse warning stimuli of 4 dB above background noise.

(E) Rotarod performance is impaired in *mHtt-Tg* mice, which is reversed by *p53* deletion. Bars indicate mean latency to fall on the accelerating rotarod ± SEM (from 4 rpm to 40 rpm over 10 min).

(F) By cross-breeding with *p53* knockout mice, the levels of mouse prion promoter (MoPrP)-driven mHtt in *mHtt-Tg* mice are not altered.

(G) Body weights of *mHtt-Tg* mice are unaffected by *p53* deletion.

All the graphs represent two independent experiments (one-way ANOVA: *$p < 0.05$). Six or seven mice were used for each genotype.

elicits increases in the levels of p53 protein in the nucleus and p53 transcriptional activity. These elevations occur in PC12 cells, primary neuronal cultures, *mHtt-Tg* mice, and postmortem brains of HD patients. Perturbation of p53 by pifithrin-α, RNAi, or genetic deletion prevents mHtt-induced cellular dysfunction and abnormal behavior in vivo. Mitochondrial membrane depolarization and cytotoxicity by mHtt is prevented by inhibition of p53. By contrast, mHtt nuclear and cytoplasmic aggregates are not influenced by *p53* deletion. Genetic deletion of *p53* suppresses mHtt-induced neurodegeneration in *Drosophila*. Some of the neurobehavioral defects in *mHtt-Tg* mice, including dyskinesia of the hindlimbs, rotational activity, prepulse inhibition, and rotarod performance, are prevented by genetic deletion of *p53*.

Increased Nuclear p53 Selectively Elicited by mHtt

We show that Htt and p53 bind in 293T cells transfected with N171 or FL Htt (Figures 1G and 1H) and in HD patient lymphoblasts (Figure 1I), consistent with in vitro binding of p53 and Htt (Figure 1F) (Steffan et al., 2000). The binding of Htt and p53 is augmented by expansion of polyQ (Figures 1F–1H). Conceivably, mHtt disturbs interactions of p53 with its regulatory proteins, such as MDM2, resulting in stabilization of p53. There is precedence for modulation of p53 function by influencing p53-MDM2 interactions, such as the stabilization of p53 by HIF-1α (Chen et al., 2003).

The stabilization and augmentation of p53 by mHtt appears to be selective and not a general toxic effect of expanded polyQ. Thus, mutant ataxin-1 with the same polyQ length fails to influence p53-mediated gene transcription. *p53* deletion does not affect the impaired motor coordination or reduced Purkinje cell number in SCA1 mice, though some later pathological features are slightly improved (Shahbazian et al., 2001). Contrast between SCA1 and *mHtt-Tg* mice may reflect p53-induced mitochondrial dysfunction in the pathology. HD lymphoblasts are highly susceptible to cyanide- or staurosporine-induced mitochondrial membrane depolarization, while SCA1 and control lymphoblasts are not (Sawa et al., 1999). Consistent with this observation, we have recently observed that UVB irradiation induces the p53 signaling cascade selectively in the fibroblasts of the patients with HD, but not in those with the other polyQ diseases, including SCA1 (unpublished data). The specificity of p53 in HD is further supported by the observation that kainate induces a lesser increase in p53 than mHtt, even though it causes more neuronal death.

In mHtt-expressing cells, we observe increases of p53-mediated gene expression and some downstream targets of p53 at the protein level. In contrast, Thompson and colleagues (Steffan et al., 2000) reported repression of p53-regulated promoters by mHtt in a *p53*-deficient human osteogenic sarcoma cell line, SAOS-2, transfected with exogenous *p53*. The two contradictory results are difficult to compare because, in the presence of mHtt, exogenous p53 in osteogenic sarcoma cells may behave differently from endogenous p53 in neurons.

Nuclear dysfunction has been implicated in HD pathophysiology. Besides p53, other nuclear transcriptional factors such as CBP (Nucifora et al., 2001), Sp1

(Dunah et al., 2002), and TAFII130 (Shimohata et al., 2000) may be involved in HD pathogenesis. For CBP, Sp1, and TAFII130, loss of function is associated with mHtt, though these studies employed cultured cells without evidence for abnormal function in intact animals. By contrast, our findings link gain of p53 function with HD in cellular and animal models as well as HD autopsy brains.

Mitochondrial Dysfunction Mediated by p53 in HD

What downstream pathways might mediate mHtt-p53-associated disturbances of mitochondrial function? p53 induces the expression of some downstream targets, such as Bax and Puma, which may lead to mitochondrial membrane depolarization (Vogelstein et al., 2000), at least in HD cell models. p53 may also regulate reactive oxygen species (ROS) levels through $p66^{SHC}$ (Sharpless and DePinho, 2002). ROS inhibit Fe-S cluster-containing enzymes, such as aconitase, and mitochondrial respiratory complexes, especially II/III and IV in HD brains (Grunewald and Beal, 1999). These disturbances can elicit mitochondrial membrane depolarization, which is evident in the neurons expressing mHtt and HD lymphoblasts.

Mitochondrial abnormalities lead to elevation of intracellular calcium concentration, which is evident in *mHtt-Tg* mice (Hansson et al., 2001; Hodgson et al., 1999). In PC12 cells expressing mHtt, we observe elevated intracellular calcium levels that are lowered by the p53 inhibitor pifithrin-α (B.-I.B., S.H.S. and A.S., unpublished data). Elevated cytosolic calcium can elicit several cellular alterations, including overactivation of the calcium-dependent protease calpain. Interestingly, cleavage of Htt by calpain is reported in HD brains (Gafni and Ellerby, 2002; Kim et al., 2001). Abnormal calcium homeostasis may link altered synaptic functions and excitotoxicity with HD mitochondrial dysfunction (Grunewald and Beal, 1999). In *mHtt-Tg* mice, increased calcium influx via medium spiny neuron-specific NR1A/NR2B-subtype NMDA receptors disturbs intracellular calcium homeostasis (Zeron et al., 2002), which can depolarize mitochondria primarily or secondarily. *p53*, synergistically upregulated by mHtt and excitotoxicity, may serve as a modulator of excitotoxicity-induced calcium abnormalities. Indeed, NMDA receptor-mediated death of striatal neurons is selectively amplified in *mHtt-Tg* mice (Zeron et al., 2002).

Influence of p53 in HD Pathogenesis In Vivo

We have shown that p53 plays a specific role in HD pathology by using *mHtt-Tg* fly and mouse models. In *Drosophila*, deletion of *p53* provides strong protection from neurotoxicity associated with the *mHtt* transgene. The protection is specific, as expression of an anti-apoptotic protein, p35, in the *mHtt-Tg* fly does not reverse its retinal degeneration (Jackson et al., 1998). In mice, pharmacologic or genetic suppression of p53 in *mHtt-Tg* normalizes respiratory complex IV activity in mitochondria and ameliorates several behavioral deficits typical of HD. Together, these results suggest that p53 may modulate mitochondrial dysfunction, cell death, and behavioral abnormalities associated with HD in vivo.

p53 in Neurological Diseases

In summary, our study establishes a specific role for p53 in HD. As p53 is a nuclear transcription factor that regulates various mitochondrial genes and insofar as mitochondrial dysfunction appears important in HD, our findings provide a molecular mechanism linking disturbances of nuclei and mitochondria in HD.

Molecular mechanisms of neurodegenerative diseases are complex (Beal, 2001; McNaught et al., 2001). Some neurological conditions display primary mitochondrial abnormalities. Mitochondrial malfunction and proteasomal disturbances have been implicated in the pathophysiology of Parkinson's disease (PD) (Beal, 2001). As p53 is regulated by its proteolysis via the ubiquitin/proteasome cascade, p53 may link proteasomal and mitochondrial abnormalities in certain forms of PD (Duan et al., 2002; Mandir et al., 2002). Though controversial, p53 has been implicated in amyotrophic lateral sclerosis (ALS) (Gonzalez de Aguilar et al., 2000; Kuntz et al., 2000). p53 is upregulated in Angelman syndrome, a neurodevelopmental disorder in which E6-AP ubiquitin ligase, which mediates p53 degradation, is mutated (Jiang et al., 1998). p53 is a nodal protein activated and stabilized by diverse mechanisms, which influences numerous downstream molecules in a context-dependent manner (Vogelstein et al., 2000). It may be rewarding to analyze features of the p53 pathway unique to each neurological disease as well as those that are shared.

A lower incidence of cancer has been reported in HD patients (Sorensen et al., 1999). As p53 is a tumor suppressor, its upregulation in multiple HD tissues might account for diminished carcinogenesis, though dietary and other extrinsic factors in cancer incidence must be ruled out (Kazemi-Esfarjani and Benzer, 2002).

Experimental Procedures

Reagents and Plasmids

Unless otherwise noted, reagents were obtained from Sigma. All the *Htt* plasmids were previously described (Cooper et al., 1998). pSuper-p53 plasmids were made as previously described (Brummelkamp et al., 2002). The targeting sequence of pSuper-p53 is the coding regions 767–787 of *R. norvegicus p53*, AAGACTCCAGTGG GAATCTTC (NM_030989), as PC12 cells were derived from rat. The targeting sequence of pSuper-control is the coding regions 773–793 of *H. sapiens p53*, AAGACTCCAGTGGTAATCTAC (NM_000546).

Immunoblotting, Co-IP, and In Vitro Binding

PC12 cells were harvested 6–8 days after the induction of Htt. For subcellular fractionation (Figure 1A), cells were homogenized with a glass-glass homogenizer (Wheaton) in 50 mM Tris-Cl buffer (pH 7.4) containing 0.32 M sucrose and protease inhibitor cocktail (Roche). Homogenates were centrifuged for 10 min at 1000 × g providing pellet (P1) and supernatant (S1). Protein concentration was measured with BCA protein assay reagent (Pierce). Equal amounts of protein were loaded and separated by SDS-PAGE. To check if p53 protein level is differentially increased in SDS-soluble or -insoluble fractions (Figure 1C), PC12 cells were homogenized in 50 mM Tris-Cl buffer (pH 7.4), 1% Triton X-100, and protease inhibitor cocktail. The homogenate was centrifuged for 30 min at 15,000 × g. The pellet was resuspended in 50 mM Tris (pH 7.4) with 1% SDS and considered total protein. After boiling for 5 min, samples were centrifuged at 1000 × g for 1 min. The loose pellet was considered the SDS-insoluble fraction, and the supernatant was considered the SDS-soluble fraction. Equal amounts of protein were analyzed by SDS-PAGE and immunoblotting. p53 protein

levels were measured in brain tissues from 8-month-old line 6 *mHtt* transgenic mice and HD patients of various Vonsattel grades (Figures 1D and 1E). For p53 positive control, wt mice received kainate (35 mg/kg i.p.) and were sacrificed after 48 hr. Striatum was dissected and used for immunoblotting. J.C. Troncoso provided human cerebral cortical, striatal, and cerebellar tissues (Vonsattel grades 1–4) from HD patients and age-matched controls (three patients per grade). All brain tissues were homogenized in RIPA lysis buffer (150 mM NaCl, 1% NP-40, 0.5% sodium deoxycholate, 0.1% SDS, and 50 mM Tris-Cl, pH 8.0). The homogenate was put on ice for 30 min and centrifuged for 10 min at 15,000 × g. The pellet was resuspended in RIPA buffer and boiled for 5 min. Samples were centrifuged at 1000 × g for 1 min, and the supernatant was used for immunoblotting. p53 (DO-1) and β-actin antibodies were from Santa Cruz. For secondary antibody and detection, VECTASTAIN Elite ABC-Kit (Vector) and SuperSignal West Femto Substrate (Pierce) were used according to the manufacturer's protocol. p53 targets were analyzed by immunoblotting using Apaf-1, Bax, and Puma antibodies (Cell Signaling) from PC12 cells transiently transfected with N171 *Htt* 90 hr after transfection (Figure 2F). To examine mHtt and p53 protein levels in the cross-bred mice (Figure 6F), brain samples were prepared from 4-month-old wt, *p53*$^{-/-}$, *mHtt-Tg*, and *mHtt-Tg/p53*$^{-/-}$ mice and immunoblotted with p53 (DO-1) and Htt (EM48; Chemicon) antibodies. For co-IP of endogenous mHtt and p53 (Figure 1I), p53 was immunoprecipitated from the RIPA lysates of HD patient lymphoblasts treated with 1 μM staurosporine for 24 hr, and Htt was immunoblotted by EM48. To evaluate the effect of polyQ expansion on the interaction (Figures 1G and 1H), co-IP of Htt and p53 was performed in 293T cells transfected with *Htt*. DO-1, EM48, and rabbit polyclonal AP231 (Htt) antibodies were used. In vitro binding of His-tagged Htt and GST-p53 proteins was performed as previously described (Li et al., 2002).

Reverse Northern Assay

We spotted 1 μg of DNAs corresponding to the open reading frame of p53, *β-actin*, *zif268*, *Fos-B*, and *Siah* genes onto a nitrocellulose membrane under the vacuum. The DNA samples were initially denatured by high concentration of NaOH at 100°C for 5 min and then were applied onto a membrane using a Bio-Rad Bio-dot microfiltration apparatus. Total mRNA was extracted from PC12 cells harvested 6–8 days after the induction of Htt and was reverse transcribed with [^{32}P]dCTP. The ^{32}P-labeled cDNA mixtures were denatured by incubation at 94°C for 5 min and rapidly chilled on ice. The membrane with spotted genes was prehybridized with heat-denatured sheared salmon sperm DNA for 1–2 hr. Then, ^{32}P-labeled cDNA probe was added to the membrane, incubated overnight at 60°C, and then washed in the next morning. Signals from the membrane were recorded on a phosphorimager.

Culture and Transfection of Primary Neocortical Neurons

E16–E18 primary neocortical cultures were prepared with mouse embryos from *p53*$^{+/-}$ × *p53*$^{+/-}$ parents of C57BL/6 strain or Sprague-Dawley rat embryos. Because *p53*$^{-/-}$ female mice are sterile, we always crossbred *p53*$^{+/-}$ males with *p53*$^{+/-}$ females and cultured embryonic neurons individually without knowing the genotype. Neurons were grown on poly-D-lysine-coated plates at 500 cells/mm^2 in Neurobasal medium with B27 supplement and 0.5 mM L-glutamine (Invitrogen). On 5 DIV or earlier, neurons were transfected with DNA using Lipofectamine 2000 (Invitrogen) following the manufacturer's protocol. Transfection efficiency was consistently 3%–5%, which was adequate for the neuron-based experiments including p53 reporter assays. Transfection efficiency was decreased dramatically after 5 DIV, so transfection was always performed on 5 DIV or earlier. The ratio of plasmid to Lipofectamine 2000 was 1:2.5. To do the experiments in a blinded manner, each mouse embryo from *p53*$^{+/-}$ × *p53*$^{+/-}$ parents was genotyped after all the analyses had been finished.

p53 Reporter Assay

All the cells used in p53 reporter assays with NGF-differentiated PC12 cells and primary neurons were plated on 35 mm dishes at a density of 10^6 cells/well and transfected within 5 days using 4 μg of DNA, 10 μl Lipofectamine 2000, and 500 μl of OPTI-MEM (Invitrogen) per well. The p53 reporter contains a consensus p53 binding site followed by luciferase (el-Deiry et al., 1992). β-galactosidase is under the control of a TK promoter. NGF-differentiated PC12 cells stably expressing Htt N63 were transfected with 3 μg of p53 reporter and 1 μg of *β-galactosidase* after 1 day of *Htt* induction (Figure 2A). 2 μg of Htt N171-18Q or N171-82Q, 1.5 μg of p53 reporter, and 0.5 μg of *β-galactosidase* were added to the rat primary neurons (Figure 2B). The luciferase assay was sensitive enough to detect differences in the 3%–5% transfected primary cortical neurons. To compare the effects of Htt and ataxin-1 on p53 transcriptional activity (Figure 2C), NGF-differentiated normal PC12 cells were transfected with 2 μg of *Htt* N171-18Q, N171-82Q, full-length *Htt* with 23Q (FL-23Q), FL-82Q, *ataxin-1*-2Q, or *ataxin-1*-82Q, plus 1.5 μg of p53 reporter and 0.5 μg of *β-galactosidase*. For the pifithrin-α experiment (Figure 2E), NGF-differentiated normal PC12 cells were transfected with 2 μg of *Htt* N171-18Q or N171-82Q, 1.5 μg of p53 reporter and 0.5 μg of *β-galactosidase*, and 1 μM pifithrin-α or DMSO was added simultaneously. For the RNAi experiment (Figure 2E), PC12 cells were transfected with 1.2 μg of pSuper-control or pSuper-p53, 0.6 μg of *Htt* N171, 0.15 μg of p53 reporter, and 0.05 μg of *β-galactosidase*, and harvested after 72 hr of transfection. Luciferase activity was measured using the Promega Luciferase Assay System following the manufacturer's protocol and normalized to β-galactosidase activity or total protein concentration, both of which gave identical results.

Mitochondrial Depolarization Assay and Respiratory Chain Complex IV Activity Assay

Mitochondrial membrane potential was measured in lymphoblasts from the HD patients or control subjects as previously described (Sawa et al., 1999). Pifithrin-α (10 μM) was added to the lymphoblasts 24 hr before 25 μM cyanide exposure. Mitochondrial membrane potential of PC12 cells and primary neurons expressing Htt was examined with JC-1 and Mitotracker (Molecular Probes), respectively, following the manufacturer's protocol. PC12 cells were observed using a Perkin Elmer UltraVIEW confocal microscope, while for primary neurons, a Zeiss Axiovert 135 microscope was employed. Exposure time was constant throughout the procedure. To induce rapid mitochondrial depolarization in PC12 cells, 50 μM FCCP was applied for 10 min after 5 min plasma membrane permeabilization by 0.01% w/v digitonin in 130 mM KCl, 5 mM HEPES (pH 7.0), and 5 mM glutamate. Each graph bar corresponds to the scoring of 500 PC12 cells or 1000 to 2000 primary neurons from randomly chosen fields. Mitochondrial respiratory chain complex IV, cytochrome C oxidase, activity in mouse striatum was measured as previously described (Tabrizi et al., 2000). Line 81 *mHtt-Tg* mice received pifithrin-α (2 mg/kg i.p.) or DMSO daily from 2.5 months of age. *mHtt-Tg* mice and age-matched control mice were sacrificed at 5 months of age. Striatum was dissected and used for the assay of cytochrome C oxidase activity.

Viability Assay and Aggregate Formation Assay

For PC12 cells stably transfected with inducible Htt, pifithrin-α (1-10 μM) was dissolved in DMSO and added directly to the medium at the final concentration on the day of induction and every 3 days thereafter (Figure 4A). For the RNAi experiment, differentiated PC12 cells on 35 mm dishes were transiently transfected with 1 μg of *Htt* and 3 μg of pSuper-p53 or pSuper-control (Figure 4A). Cell viability was monitored using two fluorescent dyes for nuclear staining with a Zeiss Axiovert 135 inverted microscope: cell-permeable Hoechst 33258 (10 μg/ml) to label total cells, and cell-impermeable propidium iodide (10 μg/ml) for dead cells (Molecular Probes). Each experiment contained cells from ten randomly selected fields from each of two wells. The ratio of dead cells to total cells was used for statistical analysis. The result is consistent with the previous report (Igarashi et al., 2003), in which a trypan blue exclusion assay was used.

Neuronal death was quantified at 96 hr in a blinded manner as previously described (Nucifora et al., 2001). Briefly, cells with both degenerated neurites and shrunken nuclei were considered dead. Morphology of neurites and nuclei was monitored, respectively, by GFP signal and Hoechst staining. Genotyping of each set of neurons was performed after counting as described below. For mHtt

aggregate formation, N67-104Q-GFP was transfected into mouse embryonic neurons. Nuclear and cytoplasmic aggregates were scored after 2 days. Aggregates were visualized by GFP. Both epifluorescent and bright-field images were taken from the same field. Cellular compartmentalization was determined by overlaying GFP, Hoechst, and bright-field images.

Drosophila Genetics

The flies used for the morphological analyses were reared on standard *Drosophila* medium at 25°C under a 12 hr light/12 hr dark cycle. The wild-type flies used in this study were Canton S strain. *mHtt-Tg* flies (*pGMR:Htt^{Q120}*) were described previously (Jackson et al., 1998). The *pGMR:Htt^{Q120};P53^{5A-1-4}* flies were generated by genetically introducing the Htt transgene into a *P53^{5A-1-4}* background (Bloomington stock 6815). To assay the time course of retinal degeneration, the mean number of rhabdomeres per ommatidium was determined using the optical neutralization technique as previously described (Xu et al., 2004). Each data point was based on the examination of $\geq$100 ommatidia from at least five flies for *pGMR:Htt^{Q120}* and *pGMR:Htt^{Q120};P53^{5A-1-4}* flies, or $\geq$ 80 ommatidia from at least five flies for wild-type and *P53^{5A-1-4}* flies.

Mouse Maintenance and Behavioral Assay

B6C3F1/J line 81 *mHtt-Tg* mice were genotyped as previously described (Schilling et al., 1999). C57BL/6 *p53$^{+/-}$* mice were purchased from Taconic. The wild-type allele of *p53* was genotyped by PCR with 5′-GTGCAGTTGTGGGTCAGCGCCACACCTCCA-3′ and 5′-CTGTCTTCCAGATACTCGGGATAC-3′ and knockout allele, 5′-TCGTGCTTTACGGTATCGCCGCTCCCGATT-3′ and 5′-CTGTCTT CCAGATACTCGGGATAC-3′. Two *mHtt-Tg* male mice were crossed with four C57BL/6 *p53$^{+/-}$* female mice to obtain *mHtt-Tg/p53$^{+/-}$* mice. Seven *mHtt-Tg/p53$^{+/-}$* male mice were then backcrossed with 16 C57BL/6 *p53$^{+/-}$* female mice. After the double cross-breeding, 17 wt, 28 *p53$^{-/-}$*, 11 *p53$^{-/-}$*, 6 *mHtt-Tg*, 17 *mHtt-Tg/p53$^{+/-}$*, and 7 *mHtt-Tg/p53$^{-/-}$* mice were obtained. Only wt, *p53$^{-/-}$*, *mHtt-Tg*, and *mHtt-Tg/p53$^{-/-}$* mice were chosen for the behavioral assays, because *p53$^{+/-}$* mice might show marked variation in protein expression levels of posttranslationally regulated p53 in the brain. Onset of HD behavioral symptoms occurs around 3 months in line 81 *mHtt-Tg*, and robust tumorigenesis occurs after 6 months of age in *p53$^{-/-}$* mice (Donehower et al., 1992). All the behavioral analyses were performed between 3 and 4 months of age. Open-field tests were performed using a Versamax Animal Activity Monitoring System (Accuscan) for 20 hr from 4 PM to 12 PM with a dark period from 6 PM to 6 AM. Acoustic startle and prepulse inhibition responses were measured in a startle chamber (San Diego Instruments). The protocol was as reported (Carter et al., 1999) except that prepulse warnings of 2 and 4 dB above background noise and acoustic stimuli of 120 dB were adopted. Rotarod test was performed as previously reported (Schilling et al., 1999). Latency to clasping of the hindlimbs was also measured.

Densitometry and Statistical Analysis

Quantitative densitometric measurement of immunoblotting and reverse Northern assay was performed using EagleSight program (Stratagene). The results were quantified in arbitrary units, where 1 equals the level of control or wtHtt. Two-tailed p values were calculated by Student's t test and one-way analysis of variance (ANOVA) using Minitab 13. Values depicted are mean ± SEM.

Acknowledgments

We thank B. Vogelstein and K.W. Kinzler for providing p53 reporter plasmid, discussion, and critical reading of the manuscript; H.Y. Zoghbi for providing SCA1 lymphoblasts and *ataxin-1* plasmids; L.M. Thompson for critical reading of the manuscript; A. Kazantsev for providing N67-104Q-GFP plasmid; M.P. Mattson for providing pifithrin-α and discussion; J.C. Troncoso for providing postmortem HD brain tissues and discussion; X.J. Li for providing His-*Htt* N171-23Q/120Q plasmids and discussion on purifying mHtt from bacteria; D.R. Borchelt, G. Schilling, E. O'Hearn, M.E. Molliver, and R.L. Margolis for helpful discussion; L. Hester for neuronal culture; K. Nakaso, Y. Ozeki, and L. Cohen for technical help. B.-I.B. thanks J.-J. Chung and B.S.-J. Bae for unwavering support and encouragement. Supported by USPHS grants, MH-069853 (A.S.), EY08117 (C.M.), DA-00266 (S.H.S.), DA-00074 (S.H.S.); foundation grants (A.S.), Huntington's Disease Society for America grant, Hereditary Disease Foundation grant, Stanley, NARSAD award, S-R; Korea Foundation for Advanced Studies Predoctoral Fellowship (B.-I.B). The authors declare that they have no competing financial interests.

Received: October 3, 2003
Revised: December 6, 2004
Accepted: June 6, 2005
Published: July 6, 2005

References

Arrasate, M., Mitra, S., Schweitzer, E.S., Segal, M.R., and Finkbeiner, S. (2004). Inclusion body formation reduces levels of mutant huntingtin and the risk of neuronal death. Nature *431*, 805–810.

Beal, M.F. (2001). Experimental models of Parkinson's disease. Nat. Rev. Neurosci. *2*, 325–334.

Beal, M.F., Brouillet, E., Jenkins, B.G., Ferrante, R.J., Kowall, N.W., Miller, J.M., Storey, E., Srivastava, R., Rosen, B.R., and Hyman, B.T. (1993). Neurochemical and histologic characterization of striatal excitotoxic lesions produced by the mitochondrial toxin 3-nitropropionic acid. J. Neurosci. *13*, 4181–4192.

Braff, D.L., Geyer, M.A., and Swerdlow, N.R. (2001). Human studies of prepulse inhibition of startle: normal subjects, patient groups, and pharmacological studies. Psychopharmacology (Berl.) *156*, 234–258.

Browne, S.E., Bowling, A.C., MacGarvey, U., Baik, M.J., Berger, S.C., Muqit, M.M., Bird, E.D., and Beal, M.F. (1997). Oxidative damage and metabolic dysfunction in Huntington's disease: selective vulnerability of the basal ganglia. Ann. Neurol. *41*, 646–653.

Brummelkamp, T.R., Bernards, R., and Agami, R. (2002). A system for stable expression of short interfering RNAs in mammalian cells. Science *296*, 550–553.

Carter, R.J., Lione, L.A., Humby, T., Mangiarini, L., Mahal, A., Bates, G.P., Dunnett, S.B., and Morton, A.J. (1999). Characterization of progressive motor deficits in mice transgenic for the human Huntington's disease mutation. J. Neurosci. *19*, 3248–3257.

Chen, D., Li, M., Luo, J., and Gu, W. (2003). Direct interactions between HIF-1 alpha and Mdm2 modulate p53 function. J. Biol. Chem. *278*, 13595–13598.

Chipuk, J.E., Kuwana, T., Bouchier-Hayes, L., Droin, N.M., Newmeyer, D.D., Schuler, M., and Green, D.R. (2004). Direct activation of Bax by p53 mediates mitochondrial membrane permeabilization and apoptosis. Science *303*, 1010–1014.

Cooper, J.K., Schilling, G., Peters, M.F., Herring, W.J., Sharp, A.H., Kaminsky, Z., Masone, J., Khan, F.A., Delanoy, M., Borchelt, D.R., et al. (1998). Truncated N-terminal fragments of huntingtin with expanded glutamine repeats form nuclear and cytoplasmic aggregates in cell culture. Hum. Mol. Genet. *7*, 783–790.

Crawley, J.N. (2000). What's Wrong with My Mouse?: Behavioral Phenotyping of Transgenic and Knockout Mice (New York: Wiley-Liss).

DiFiglia, M., Sapp, E., Chase, K.O., Davies, S.W., Bates, G.P., Vonsattel, J.P., and Aronin, N. (1997). Aggregation of huntingtin in neuronal intranuclear inclusions and dystrophic neurites in brain. Science *277*, 1990–1993.

Donehower, L.A., Harvey, M., Slagle, B.L., McArthur, M.J., Montgomery, C.A., Jr., Butel, J.S., and Bradley, A. (1992). Mice deficient for p53 are developmentally normal but susceptible to spontaneous tumours. Nature *356*, 215–221.

Duan, W., Zhu, X., Ladenheim, B., Yu, Q.S., Guo, Z., Oyler, J., Cutler, R.G., Cadet, J.L., Greig, N.H., and Mattson, M.P. (2002). p53 inhibitors preserve dopamine neurons and motor function in experimental parkinsonism. Ann. Neurol. *52*, 597–606.

Dunah, A.W., Jeong, H., Griffin, A., Kim, Y.M., Standaert, D.G., Hersch, S.M., Mouradian, M.M., Young, A.B., Tanese, N., and

Krainc, D. (2002). Sp1 and TAFII130 transcriptional activity disrupted in early Huntington's disease. Science *296*, 2238–2243.

el-Deiry, W.S., Kern, S.E., Pietenpol, J.A., Kinzler, K.W., and Vogelstein, B. (1992). Definition of a consensus binding site for p53. Nat. Genet. *1*, 45–49.

Gafni, J., and Ellerby, L.M. (2002). Calpain activation in Huntington's disease. J. Neurosci. *22*, 4842–4849.

Gonzalez de Aguilar, J.L., Gordon, J.W., Rene, F., de Tapia, M., Lutz-Bucher, B., Gaiddon, C., and Loeffler, J.P. (2000). Alteration of the Bcl-x/Bax ratio in a transgenic mouse model of amyotrophic lateral sclerosis: evidence for the implication of the p53 signaling pathway. Neurobiol. Dis. *7*, 406–415.

Grunewald, T., and Beal, M.F. (1999). Bioenergetics in Huntington's disease. Ann. N Y Acad. Sci. *893*, 203–213.

Hackam, A.S., Singaraja, R., Wellington, C.L., Metzler, M., McCutcheon, K., Zhang, T., Kalchman, M., and Hayden, M.R. (1998). The influence of huntingtin protein size on nuclear localization and cellular toxicity. J. Cell Biol. *141*, 1097–1105.

Hansson, O., Guatteo, E., Mercuri, N.B., Bernardi, G., Li, X.J., Castilho, R.F., and Brundin, P. (2001). Resistance to NMDA toxicity correlates with appearance of nuclear inclusions, behavioural deficits and changes in calcium homeostasis in mice transgenic for exon 1 of the huntington gene. Eur. J. Neurosci. *14*, 1492–1504.

Hay, B.A., Wolff, T., and Rubin, G.M. (1994). Expression of baculovirus P35 prevents cell death in Drosophila. Development *120*, 2121–2129.

Hebb, M.O., and Robertson, H.A. (1999). Motor effects and mapping of cerebral alterations in animal models of Parkinson's and Huntington's diseases. J. Comp. Neurol. *410*, 99–114.

Hodgson, J.G., Agopyan, N., Gutekunst, C.A., Leavitt, B.R., LePiane, F., Singaraja, R., Smith, D.J., Bissada, N., McCutcheon, K., Nasir, J., et al. (1999). A YAC mouse model for Huntington's disease with full-length mutant huntingtin, cytoplasmic toxicity, and selective striatal neurodegeneration. Neuron *23*, 181–192.

The Huntington's Disease Collaborative Research Group. (1993). A novel gene containing a trinucleotide repeat that is expanded and unstable on Huntington's disease chromosomes. Cell *72*, 971–983.

Igarashi, S., Morita, H., Bennett, K.M., Tanaka, Y., Engelender, S., Peters, M.F., Cooper, J.K., Wood, J.D., Sawa, A., and Ross, C.A. (2003). Inducible PC12 cell model of Huntington's disease shows toxicity and decreased histone acetylation. Neuroreport *14*, 565–568.

Jackson, G.R., Salecker, I., Dong, X., Yao, X., Arnheim, N., Faber, P.W., MacDonald, M.E., and Zipursky, S.L. (1998). Polyglutamine-expanded human huntingtin transgenes induce degeneration of Drosophila photoreceptor neurons. Neuron *21*, 633–642.

Jiang, Y.H., Armstrong, D., Albrecht, U., Atkins, C.M., Noebels, J.L., Eichele, G., Sweatt, J.D., and Beaudet, A.L. (1998). Mutation of the Angelman ubiquitin ligase in mice causes increased cytoplasmic p53 and deficits of contextual learning and long-term potentiation. Neuron *21*, 799–811.

Jordan, J., Galindo, M.F., Prehn, J.H., Weichselbaum, R.R., Beckett, M., Ghadge, G.D., Roos, R.P., Leiden, J.M., and Miller, R.J. (1997). p53 expression induces apoptosis in hippocampal pyramidal neuron cultures. J. Neurosci. *17*, 1397–1405.

Kazemi-Esfarjani, P., and Benzer, S. (2002). Suppression of polyglutamine toxicity by a Drosophila homolog of myeloid leukemia factor 1. Hum. Mol. Genet. *11*, 2657–2672.

Kim, Y.J., Yi, Y., Sapp, E., Wang, Y., Cuiffo, B., Kegel, K.B., Qin, Z.H., Aronin, N., and DiFiglia, M. (2001). Caspase 3-cleaved N-terminal fragments of wild-type and mutant huntingtin are present in normal and Huntington's disease brains, associate with membranes, and undergo calpain-dependent proteolysis. Proc. Natl. Acad. Sci. USA *98*, 12784–12789.

Komarov, P.G., Komarova, E.A., Kondratov, R.V., Christov-Tselkov, K., Coon, J.S., Chernov, M.V., and Gudkov, A.V. (1999). A chemical inhibitor of p53 that protects mice from the side effects of cancer therapy. Science *285*, 1733–1737.

Kuntz, C., 4th, Kinoshita, Y., Donehower, L.A., and Morrison, R.S. (2000). Absence of p53: no effect in a transgenic mouse model of familial amyotrophic lateral sclerosis. Exp. Neurol. *165*, 184–190.

Li, S.H., Cheng, A.L., Zhou, H., Lam, S., Rao, M., Li, H., and Li, X.J. (2002). Interaction of Huntington disease protein with transcriptional activator Sp1. Mol. Cell. Biol. *22*, 1277–1287.

Mandir, A.S., Simbulan-Rosenthal, C.M., Poitras, M.F., Lumpkin, J.R., Dawson, V.L., Smulson, M.E., and Dawson, T.M. (2002). A novel in vivo post-translational modification of p53 by PARP-1 in MPTP-induced parkinsonism. J. Neurochem. *83*, 186–192.

Marsh, J.L., Walker, H., Theisen, H., Zhu, Y.Z., Fielder, T., Purcell, J., and Thompson, L.M. (2000). Expanded polyglutamine peptides alone are intrinsically cytotoxic and cause neurodegeneration in Drosophila. Hum. Mol. Genet. *9*, 13–25.

McNaught, K.S., Olanow, C.W., Halliwell, B., Isacson, O., and Jenner, P. (2001). Failure of the ubiquitin-proteasome system in Parkinson's disease. Nat. Rev. Neurosci. *2*, 589–594.

Miyashita, T., and Reed, J.C. (1995). Tumor suppressor p53 is a direct transcriptional activator of the human bax gene. Cell *80*, 293–299.

Morrison, R.S., and Kinoshita, Y. (2000). The role of p53 in neuronal cell death. Cell Death Differ. *7*, 868–879.

Morrison, R.S., Wenzel, H.J., Kinoshita, Y., Robbins, C.A., Donehower, L.A., and Schwartzkroin, P.A. (1996). Loss of the p53 tumor suppressor gene protects neurons from kainate-induced cell death. J. Neurosci. *16*, 1337–1345.

Nucifora, F.C., Jr., Sasaki, M., Peters, M.F., Huang, H., Cooper, J.K., Yamada, M., Takahashi, H., Tsuji, S., Troncoso, J., Dawson, V.L., et al. (2001). Interference by huntingtin and atrophin-1 with cbp-mediated transcription leading to cellular toxicity. Science *291*, 2423–2428.

Panov, A.V., Gutekunst, C.A., Leavitt, B.R., Hayden, M.R., Burke, J.R., Strittmatter, W.J., and Greenamyre, J.T. (2002). Early mitochondrial calcium defects in Huntington's disease are a direct effect of polyglutamines. Nat. Neurosci. *5*, 731–736.

Peters, M.F., Nucifora, F.C., Jr., Kushi, J., Seaman, H.C., Cooper, J.K., Herring, W.J., Dawson, V.L., Dawson, T.M., and Ross, C.A. (1999). Nuclear targeting of mutant Huntingtin increases toxicity. Mol. Cell. Neurosci. *14*, 121–128.

Reddy, P.H., Williams, M., Charles, V., Garrett, L., Pike-Buchanan, L., Whetsell, W.O., Jr., Miller, G., and Tagle, D.A. (1998). Behavioural abnormalities and selective neuronal loss in HD transgenic mice expressing mutated full-length HD cDNA. Nat. Genet. *20*, 198–202.

Rong, Y.S., Titen, S.W., Xie, H.B., Golic, M.M., Bastiani, M., Bandyopadhyay, P., Olivera, B.M., Brodsky, M., Rubin, G.M., and Golic, K.G. (2002). Targeted mutagenesis by homologous recombination in D. melanogaster. Genes Dev. *16*, 1568–1581.

Ross, C.A. (2002). Polyglutamine pathogenesis: emergence of unifying mechanisms for Huntington's disease and related disorders. Neuron *35*, 819–822.

Sanchez, I., Mahlke, C., and Yuan, J. (2003). Pivotal role of oligomerization in expanded polyglutamine neurodegenerative disorders. Nature *421*, 373–379.

Sang, T.K., Li, C., Liu, W., Rodriguez, A., Abrams, J.M., Zipursky, S.L., and Jackson, G.R. (2005). Inactivation of Drosophila Apaf-1 related killer suppresses formation of polyglutamine aggregates and blocks polyglutamine pathogenesis. Hum. Mol. Genet. *14*, 357–372.

Saudou, F., Finkbeiner, S., Devys, D., and Greenberg, M.E. (1998). Huntingtin acts in the nucleus to induce apoptosis but death does not correlate with the formation of intranuclear inclusions. Cell *95*, 55–66.

Sawa, A. (2001). Mechanisms for neuronal cell death and dysfunction in Huntington's disease: pathological cross-talk between the nucleus and the mitochondria? J. Mol. Med. *79*, 375–381.

Sawa, A., Wiegand, G.W., Cooper, J., Margolis, R.L., Sharp, A.H., Lawler, J.F., Jr., Greenamyre, J.T., Snyder, S.H., and Ross, C.A. (1999). Increased apoptosis of Huntington disease lymphoblasts associated with repeat length-dependent mitochondrial depolarization. Nat. Med. *5*, 1194–1198.

Schapira, A.H. (1997). Mitochondrial function in Huntington's disease: clues for pathogenesis and prospects for treatment. Ann. Neurol. *41*, 141–142.

Schilling, G., Becher, M.W., Sharp, A.H., Jinnah, H.A., Duan, K., Kotzuk, J.A., Slunt, H.H., Ratovitski, T., Cooper, J.K., Jenkins, N.A., et al. (1999). Intranuclear inclusions and neuritic aggregates in transgenic mice expressing a mutant N-terminal fragment of huntingtin. Hum. Mol. Genet. *8*, 397–407.

Schilling, G., Savonenko, A.V., Klevytska, A., Morton, J.L., Tucker, S.M., Poirier, M., Gale, A., Chan, N., Gonzales, V., Slunt, H.H., et al. (2004). Nuclear-targeting of mutant huntingtin fragments produces Huntington's disease-like phenotypes in transgenic mice. Hum. Mol. Genet. *13*, 1599–1610.

Shahbazian, M.D., Orr, H.T., and Zoghbi, H.Y. (2001). Reduction of Purkinje cell pathology in SCA1 transgenic mice by p53 deletion. Neurobiol. Dis. *8*, 974–981.

Sharpless, N.E., and DePinho, R.A. (2002). p53: good cop/bad cop. Cell *110*, 9–12.

Shimohata, T., Nakajima, T., Yamada, M., Uchida, C., Onodera, O., Naruse, S., Kimura, T., Koide, R., Nozaki, K., Sano, Y., et al. (2000). Expanded polyglutamine stretches interact with TAFII130, interfering with CREB-dependent transcription. Nat. Genet. *26*, 29–36.

Sipione, S., Rigamonti, D., Valenza, M., Zuccato, C., Conti, L., Pritchard, J., Kooperberg, C., Olson, J.M., and Cattaneo, E. (2002). Early transcriptional profiles in huntingtin-inducible striatal cells by microarray analyses. Hum. Mol. Genet. *11*, 1953–1965.

Sisodia, S.S. (1998). Nuclear inclusions in glutamine repeat disorders: are they pernicious, coincidental, or beneficial? Cell *95*, 1–4.

Sorensen, S.A., Fenger, K., and Olsen, J.H. (1999). Significantly lower incidence of cancer among patients with Huntington disease: An apoptotic effect of an expanded polyglutamine tract? Cancer *86*, 1342–1346.

Steffan, J.S., Kazantsev, A., Spasic-Boskovic, O., Greenwald, M., Zhu, Y.Z., Gohler, H., Wanker, E.E., Bates, G.P., Housman, D.E., and Thompson, L.M. (2000). The Huntington's disease protein interacts with p53 and CREB-binding protein and represses transcription. Proc. Natl. Acad. Sci. USA *97*, 6763–6768.

Swerdlow, N.R., Paulsen, J., Braff, D.L., Butters, N., Geyer, M.A., and Swenson, M.R. (1995). Impaired prepulse inhibition of acoustic and tactile startle response in patients with Huntington's disease. J. Neurol. Neurosurg. Psychiatry *58*, 192–200.

Tabrizi, S.J., Cleeter, M.W., Xuereb, J., Taanman, J.W., Cooper, J.M., and Schapira, A.H. (1999). Biochemical abnormalities and excitotoxicity in Huntington's disease brain. Ann. Neurol. *45*, 25–32.

Tabrizi, S.J., Workman, J., Hart, P.E., Mangiarini, L., Mahal, A., Bates, G., Cooper, J.M., and Schapira, A.H. (2000). Mitochondrial dysfunction and free radical damage in the Huntington R6/2 transgenic mouse. Ann. Neurol. *47*, 80–86.

Tobin, A.J., and Signer, E.R. (2000). Huntington's disease: the challenge for cell biologists. Trends Cell Biol. *10*, 531–536.

Trettel, F., Rigamonti, D., Hilditch-Maguire, P., Wheeler, V.C., Sharp, A.H., Persichetti, F., Cattaneo, E., and MacDonald, M.E. (2000). Dominant phenotypes produced by the HD mutation in STHdh(Q111) striatal cells. Hum. Mol. Genet. *9*, 2799–2809.

Vogelstein, B., Lane, D., and Levine, A.J. (2000). Surfing the p53 network. Nature *408*, 307–310.

Wellington, C.L., Singaraja, R., Ellerby, L., Savill, J., Roy, S., Leavitt, B., Cattaneo, E., Hackam, A., Sharp, A., Thornberry, N., et al. (2000). Inhibiting caspase cleavage of huntingtin reduces toxicity and aggregate formation in neuronal and nonneuronal cells. J. Biol. Chem. *275*, 19831–19838.

Wheeler, V.C., White, J.K., Gutekunst, C.A., Vrbanac, V., Weaver, M., Li, X.J., Li, S.H., Yi, H., Vonsattel, J.P., Gusella, J.F., et al. (2000). Long glutamine tracts cause nuclear localization of a novel form of huntingtin in medium spiny striatal neurons in HdhQ92 and HdhQ111 knock-in mice. Hum. Mol. Genet. *9*, 503–513.

Xu, H., Lee, S.J., Suzuki, E., Dugan, K.D., Stoddard, A., Li, H.S., Chodosh, L.A., and Montell, C. (2004). A lysosomal tetraspanin associated with retinal degeneration identified via a genome-wide screen. EMBO J. *23*, 811–822.

Yu, J., Zhang, L., Hwang, P.M., Kinzler, K.W., and Vogelstein, B. (2001). PUMA induces the rapid apoptosis of colorectal cancer cells. Mol. Cell *7*, 673–682.

Zeron, M.M., Hansson, O., Chen, N., Wellington, C.L., Leavitt, B.R., Brundin, P., Hayden, M.R., and Raymond, L.A. (2002). Increased sensitivity to N-methyl-D-aspartate receptor-mediated excitotoxicity in a mouse model of Huntington's disease. Neuron *33*, 849–860.